Intramolecular Interaction between the DEP Domain of RGS7 and the Gβ 5 Subunit †

ARTICLE *in* BIOCHEMISTRY · JULY 2007

Impact Factor: 3.02 · DOI: 10.1021/bi700524w · Source: PubMed

Intramolecular Interaction between the DEP Domain of RGS7 and the Gβ_5 Subunit†

Vijaya Narayanan,‡ Simone L. Sandiford,‡ Qiang Wang, Tal Keren-Raifman, Konstantin Levay, and Vladlen Z. Slepak*

Department of Molecular and Cellular Pharmacology and Neuroscience Program, University of Miami, Miami, Florida 33136

Received March 15, 2007

ABSTRACT: The R7 family of RGS proteins (RGS6, -7, -9, -11) is characterized by the presence of three domains: DEP, GGL, and RGS. The RGS domain interacts with Gα subunits and exhibits GAP activity. The GGL domain permanently associates with Gβ_5. The DEP domain interacts with the membrane anchoring protein, R7BP. Here we provide evidence for a novel interaction within this complex: between the DEP domain and Gβ_5. GST fusion of the RGS7 DEP domain (GST-R7DEP) binds to both native and recombinant Gβ_5-RGS7, recombinant G$\beta\gamma$ complexes, and monomeric Gβ_5 and Gβ_1 subunits. Co-immunoprecipitation and FRET assays supported the GST pull-down experiments. GST-R7DEP reduced FRET between CFP-Gβ_5 and YFP-RGS7, indicating that the DEP-Gβ_5 interaction is dynamic. In transfected cells, R7BP had no effect on the Gβ_5/RGS7 pull down by GST-R7DEP. The DEP domain of RGS9 did not bind to Gβ_5. Substitution of RGS7 Glu-73 and Asp-74 for the corresponding Ser and Gly residues (ED/SG mutation) of RGS9 diminished the DEP-Gβ_5 interaction. In the absence of R7BP both the wild-type RGS7 and the ED/SG mutant attenuated muscarinic M3 receptor-mediated Ca^{2+} mobilization. In the presence of R7BP, wild-type RGS7 lost this inhibitory activity, whereas the ED/SG mutant remained active. Taken together, our results are consistent with the following model. The Gβ_5-RGS7 molecule can exist in two conformations: "closed" and "open", when the DEP domain and Gβ_5 subunit either do or do not interact. The closed conformation appears to be less active with respect to its effect on G_q-mediated signaling than the open conformation.

G protein mediated signaling is a major mode of signal transduction in eukaryotic cells. Binding of an agonist to a heptahelical G protein coupled receptor (GPCR) activates the heterotrimeric G protein by catalyzing the exchange of GDP for GTP on the Gα subunit. The activated G protein modulates the activity of their downstream effectors until GTP hydrolysis returns the G protein to the resting GDP-bound state. Regulators of G protein signaling (RGS)[1] constitute a diverse family of proteins which modulate this signaling cascade in many ways (*1*, *2*). They are best known for their ability to accelerate GTP hydrolysis by Gα subunits (GAP activity), which results in rapid signal turnoff (*2*, *3*). All RGS proteins contain a canonical RGS box of about 120 amino acids, which is responsible for the association with the Gα subunit. Many members of the RGS family also contain additional domains, which are responsible for the diverse functions of these molecules and on the basis of which RGSs are classified into subfamilies (*2*, *4*, *5*).

The RGS7 family of proteins (R7 family) is comprised of RGS6, -7, -9, and -11, all of which contain the C-terminal RGS box, a DEP (*D*ishevelled, *E*gl-10, *P*leckstrin) domain localized in the N-terminal part of the molecule, and a centrally positioned GGL (*G-g*amma-*l*ike) domain. In both vertebrates and invertebrates, members of this RGS family have only been found in the nervous system (*6*, *7*). It appears that each family member is expressed in distinct regions of rodent brain, with RGS7 being the most abundant and widely distributed (*8*). The most extensively studied member of the R7 family is RGS9, which is expressed as two splice versions, RGS9-1, shown to regulate rod and cone phototransduction (*9*−*13*), and RGS9-2, which regulates dopamine and opioid signaling in basal ganglia (*14*, *15*). In vitro studies have demonstrated that mammalian R7 family members possess GAP activity toward $G_{i/o}$ but not G_q family α subunits (*16*, *17*). At the same time, RGS7 has been shown to attenuate G_q-mediated Ca^{2+} mobilization in transfected cells (*18*−*21*). In *Caenorhabditis elegans*, the R7 family orthologues Egl-10 and Eat-16 regulate G_o- and G_q-mediated signaling, respectively (*22*).

A distinctive feature of R7 family RGS proteins is that they exist as stably associated heterodimers with Gβ_5; neither R7 RGS proteins nor Gβ_5 have been found apart from each other in native tissues (*20*, *23*, *24*). Similar to the R7 family RGSs, Gβ_5 has been detected only in neuronal tissues and cells (*25*−*27*). Gβ_5-RGS association requires the presence of the GGL domain, which binds with high affinity to Gβ_5 but not to other Gβ subunits (*28*−*30*). While the functional role of Gβ_5 in the dimer is still not clear (*27*, *31*, *32*), it has been established that Gβ5-RGS association is necessary for the stabilization of the heterodimer against the proteolysis,

† Supported by NIH Grant GM 060019 and American Heart Association South-East Affiliate Grant-in-Aid 0455387B to V.Z.S.

* Corresponding author. Phone: (305) 243-3430. Fax: (305) 243-4555. E-mail: v.slepak@miami.edu.

‡ These authors contributed equally to this work.

[1] Abbreviations: RGS, regulator of G protein signaling; R7BP, R7 family RGS protein binding protein; R9AP, RGS9 anchoring protein; GST, glutathione *S*-transferase; FRET, fluorescence resonance energy transfer; CFP and YFP, cyan and yellow versions of green fluorescent protein (GFP).

10.1021/bi700524w CCC: $37.00
Published on Web 05/19/2007

both in reconstituted cellular systems and in animal models (*20*, *33*−*35*).

The DEP domain was identified through sequence analysis of pleckstrin and was found to be common to many signaling proteins such as Dishevelled and Egl-10. In these proteins, the DEP domain consists of approximately 70−80 amino acids. The functions of DEP domains are poorly understood (*36*). Some sequence homology exists among the various DEP domains, and key three-dimensional features, such as the core of α helices and the β sheets, are predicted to be similar on the basis of NMR studies of Dishevelled and Pleckstrin DEP domains (*37*, *38*). A cluster of basic residues on a portion of the surface has been proposed to mediate membrane localization, and a strong electric dipole created by three charged residues on the surface of mouse Dishevelled (mDvl1) has been suggested as being responsible for mediating protein−protein interactions (*37*). Perhaps the most significant advance in understanding the role of the DEP domain in the R7 family of RGS proteins has been the discovery of membrane anchoring proteins R9AP and R7BP, both of which bind to the R7 family DEP domains (*39*). It was shown that, in addition to attaching RGS7 and RGS9 to the membranes, both R9AP and R7BP affect the regulation of G protein signaling by these RGS protein complexes (*40*−*42*). Another potential binding partner associated with RGS7 via the DEP domain is snapin, a protein associated with the SNARE complex in neurons, which was identified in a yeast two-hybrid screen with an N-terminal portion of RGS7 as the bait (*43*). This finding is particularly intriguing because R7BP and R9AP display weak similarity to SNARE proteins (*42*).

In this study, we present an unexpected finding for both the DEP domain and Gβ_5: a direct interaction between the DEP domain of RGS7 and G protein β subunits.

MATERIALS AND METHODS

Antibodies. Affinity-purified anti-peptide rabbit polyclonal antibodies raised against RGS7, RGS9, Gβ_5, and Gβ_1 have been described earlier (*20*). Antibody against GFP was from Clontech, and anti-FLAG antibody was from Sigma.

Cloning of GST-DEP Constructs. The following constructs were generated for bacterial expression and subsequent purification.

(A) GST-R7DEP. Nucleotides 100−372 (corresponding to amino acids 34−124 of bovine RGS7) were PCR amplified from full-length RGS7 using the forward primer 5′-GGAATTCATGCAAGATGAAAAAAACGGA-3′ and the reverse primer 5′-GGAAGCTTTCAGTGATGGTGATGGTGATGTTCCGGCTCCCAACAATTT-3′. This fragment was cloned into the pGEX-KG vector linearized with *Eco*RI/*Hin*dIII. The double mutation, E73S/D74G, was introduced using the forward primer 5′-AAGAACTTAACCATAAGCGGACCAGTGGAGGCACTC-3′ and the reverse primer 5′-GAGTGCCTCCACTGGTCCGCTTATGGTTAAGTTCTT-3′.

(B) GST-R9DEP. Nucleotides 163−456 (corresponding to amino acids 20−117 of bovine RGS9) were amplified using the forward primer 5′-GTGGAATTCTAATCGAGGCCCTTGTGAAGGAC-3′ and the reverse primer 5′-CACGTCGACTTCAGCCGGCCACTGCTGGG-3′. The purified DNA fragment was cloned into the pGEX-KG vector at *Eco*RI and *Sal*I sites.

Purification of GST-DEP Constructs. GST fusion proteins were expressed in *Escherichia coli* and purified on glutathione beads using a standard protocol described earlier (*44*). Briefly, 1 L bacterial cultures were grown to an OD_{600} of 1.0 at 37 °C. Protein expression was induced with the addition of 0.4 mM IPTG for 1.5−2 h at 30 °C. Cells were pelleted and stored at −70 °C until further use. Pellets were resuspended in STE (100 mM Tris-HCl, pH 8.0, 150 mM NaCl, 1 mM EDTA) buffer containing DNase, lysozyme, 5 mM DTT, and protease inhibitors. The cell suspension was briefly sonicated on ice. Sarkosyl (final concentration of 1.5%) and Triton X-100 (final concentration of 2%) were added to the cell lysate accompanied by shaking at room temperature for 1 h. Thereafter, the lysate was centrifuged at 19000 rpm at 4 °C for 30 min. The clarified lysate was batch processed using GST−Sepharose 4B beads (GE) using a standard batchwise procedure. After elution from the beads, the proteins were concentrated using a Centricon filter cartridge with a 10 kDa cutoff, desalted on Sephadex G-25 preequilibrated with buffer containing 100 mM Tris-HCl, pH 8.0, 150 mM NaCl, and 15% glycerol, and stored frozen in aliquots at −80 °C. The concentration of the frozen GST-R7DEP protein stock was 2.5 mg/mL (∼65 μM); the protein precipitated at concentrations above 100 μM. The purity of GST fusions was verified by SDS−PAGE (protein degradation products constituted less than 10% of total), and the concentration was determined using the Bio-Rad protein assay kit using bovine serum albumin as a standard. The amount of GST fusion proteins used in the pull-down assays was also verified by SDS−PAGE with subsequent Coomassie staining (for example, see Figure 7B).

Constructs for Expression in Mammalian Cells. (A) Δ*DEP-RGS7*. RGS7 cDNA was cloned into the pcDNA3 vector at *Bam*HI and *Not*I sites. A construct lacking the DEP domain, ΔDEP-RGS7, was generated using PCR mutagenesis for the removal of nucleotides 100−375 corresponding to amino acids 34−125.

(B) RGS7$^{249-469}$. This RGS7 construct, which lacks the DEP domain and the linker region, was generated by PCR amplification of nucleotides 745−1410 (corresponding to amino acids 249−469) using the forward primer 5′-CCGGATCCACCATGGAAACTAAACCTCCCACA-3′ and the reverse primer 5′-CCGCGGCCGCTTAATAAGACTGAACGAGGCT-3′. The fragment was cloned into the pcDNA3 vector linearized with *Bam*HI/*Not*I.

(C) YFP-R7$^{1-248}$. Nucleotides 1−744 (corresponding to amino acids 1−248 of the full-length bovine RGS7) were amplified using the forward primer 5′-CCAAGCTTATGCAAGATGAAAAAAACGGA-3′ and the reverse primer 5′-CTGAAGCTTTGGTGTGGGTGTGTGGGTAG-3′. The fragment was cloned into the pEYFP-N1 vector at *Hin*dIII and *Sal*I sites.

(D) Full-Length RGS7 ED/SG Mutant (RGS7$^{ED/SG}$). RGS7 cDNA was cloned into the pcDNA3 vector at *Bam*HI and *Not*I sites. The double mutation E73S/D74G was introduced using the same primers used for the GST-R7DEP double mutation.

Cell Culture and Transfection. COS-7 cells were cultured in Dulbecco's minimum essential medium supplemented with 10% fetal bovine serum and penicillin/streptomycin. CHO-K1 cells were cultured in F-12K nutrient mixture (Kaighn's modification; Gibco) with 10% fetal bovine serum and

penicillin/streptomycin. Twenty-four hours prior to transfection, the cells were plated to achieve a density of $0.8 \times 10^6-1.0 \times 10^6$ cells per 100 mm plate. Transfection was carried out using lipofectamine 2000 (Invitrogen) as per the manufacturer's instructions. The DNA ratio of RGS7 to Gβ5 was maintained at 5:1, with a total of 8.0 μg of DNA per plate. LacZ DNA was used as a control to ensure that the total DNA per plate used in the COS-7 cotransfection assays remained constant. Forty-eight hours after transfection, cells were washed with HBSS, harvested, and used for immunoprecipitation and pull-down assays or were pelleted and stored at −70 °C for use in FRET assays.

In Vitro Translation. To obtain ^{35}S-Met-labeled proteins, the rabbit reticulocyte in vitro translation/transcription system (Promega) was used according to the manufacturer's instructions as described previously (*29*).

Preparation of Brain Homogenates. Mouse brains were homogenized in lysis buffer (20 mM Tris-HCl, pH 7.5, 1 mM EDTA, 50 mM NaCl, 2 mM β-mercaptoethanol) and centrifuged at 50000*g* for 20 min at 4 °C. The pellet containing the membranes was washed and resuspended in the same buffer containing 1% sodium cholate. This suspension was left on ice for 30 min and then centrifuged at 50000*g* for 30 min, and the supernatant was used as the membrane extract.

GST Pull Down. Glutathione−Sepharose 4B beads were prewashed with PBS plus 0.1% CHAPS, incubated at 4 °C with purified recombinant GST or the GST fusion proteins for 1 h, and washed three times with PBS plus 0.1% CHAPS to remove excess protein. The slurry was incubated for 1−2 h at 4 °C on a rotary shaker with the various lysates as determined by the experiment. At the end of the incubation, the beads were settled by gravity, and the supernatant was collected as the unbound fraction. The resin was extensively washed and subsequently eluted with the addition of SDS-containing sample loading buffer. In a typical assay, the packed volume of the GST resin was 30 μL, the amount of loaded GST fusion protein was 10 μg, and the volume of the protein lysate was 300 μL. The total protein concentration in the brain or transfected cell lysates was 2.5−5.0 mg/mL. The beads were washed three times with 600 μL of PBS plus 0.1% CHAPS buffer and eluted with 30 μL of 2× SDS sample loading buffer. The unbound and eluted fractions were resolved by gel electrophoresis and analyzed by western blotting. We found that the pull-down assays worked most efficiently if the protein extracts from brain or transfected cells were prepared using 1% cholate. Triton X-100 at 0.1% nearly completely inhibited the pull down of Gβ_5-RGS7 complexes by GST-R7DEP.

Immunoprecipitation from COS-7 Cell Lysates. Forty-eight hours after transient transfection with the required constructs, COS-7 cells were washed with HBSS and then harvested in lysis buffer (20 mM Tris-HCl, pH 8.0, 100 mM NaCl, 2 mM $MgSO_4$, 5% glycerol, and protease inhibitors). The suspension was freeze−thawed, passed through a 19 gauge needle, and incubated, with shaking, at 4 °C for 1 h, and the resulting lysate was centrifuged at 14000 rpm for 30 min. The supernatant was incubated with protein A−Sepharose that had been previously washed and bound to the RGS7 antibody, as described earlier (*20*). After 2−3 h of incubation on a rotating platform at 4 °C, beads were washed and eluted with 2× SDS sample loading buffer. The unbound and immunoprecipitated fractions were analyzed by western blotting.

Confocal Microscopy. Twenty-four hours prior to transfection, cells were plated to achieve a density of 1×10^5 cells on 22 mm glass coverslips in a six-well plate. Transfection was carried out using lipofectamine 2000 (Invitrogen) as per the manufacturer's instructions. Following the transfection, the coverslips were washed twice in PBS and then fixed in 4% paraformaldehyde for 25 min at room temperature. Coverslips were then rinsed with PBS, mounted on slides for confocal microscopy, and imaged using a Zeiss LSM 510 laser scanning confocal microscope.

FRET. FRET assays were performed with transiently transfected COS-7 cell lysates. COS-7 cells were grown to 70% confluency and transfected in 100 mm plates. Cells were harvested, and the lysates were obtained using the same procedures as for immunoprecipitation and GST pull downs. Protein assays were performed to determine the total protein concentrations in the supernatants, which were then adjusted with PBS to attain the same concentration (typically, 2 mg/mL). We used two methods to study the effect of GST-R7DEP on FRET within the YFP-RGS7 and CFP-Gβ_5 fusion proteins.

In the first method (see Figure 5), FRET between CFP- and YFP-tagged proteins was determined as described in detail earlier (*21*, *45*). Briefly, the cell lysates were placed in a 4 mL quartz cuvette in a photon counting spectrofluorometer (PTI, Inc.), and the emission spectra were recorded at room temperature with continuous mixing of the lysate with a magnetic stirrer. CFP was excited at 433 nm (2−4 nm slit width, depending on the intensity of fluorescence signal), and the spectra were obtained between 465 and 555 nm. The emission peak of YFP was observed at 524−525 nm. For each recording, three spectral scans were performed to obtain the average, which was used in subsequent calculations. The following spectra were recorded. First, the spectra from the lysate containing both the CFP and YFP fusion proteins, i.e., CFP-Gβ5 and YFP-RGS7, were measured. Second, fluorescence was measured from the lysate expressing CFP-Gβ5/RGS7; this control provided us with the measure of CFP fluorescence bleed-through into the YFP emission channels. Third, fluorescence was measured from lysate expressing YFP-RGS7 alone; this was an estimation of the background excitation of YFP at 433 nm. The baseline fluorescence of the cell lysate was determined using cells containing no fluorescently tagged proteins. This "empty" spectrum was subtracted from the spectra recorded from the lysates containing the fluorescent proteins. Then, the "CFP-only" and "YFP-only" spectra were subtracted from the "CFP + YFP" spectrum to detect the increase of YFP fluorescence that occurred due to FRET. These differential spectra are presented in Figure 4. As previously described (*21*, *45*), in order to correct for the difference between the YFP level in different lysates containing the fusions, for example, CFP-Gβ_5/YFP-RGS7 and untagged Gβ_5/YFP-RGS7, the amount of YFP was determined by measuring the YFP emission when it was excited at 465 nm at which there is maximal YFP excitation. If there was a difference, it was factored into the calculation of the difference between the spectra.

In the second method, we monitored the change in fluorescence of CFP and YFP using only one cell lysate containing both the donor and acceptor, CFP-Gβ_5/YFP-

RGS7. In this simplified assay, the contribution of CFP bleed-through and background fluorescence were not determined, and therefore the actual FRET value was not calculated. Rather, we determined the specific GST-R7DEP-induced change in total fluorescence. The CFP-Gβ_5/YFP-RGS7 cell lysate was obtained from transfected COS-7 cells and split in three 2 mL aliquots. GST-R7DEP or GST stocks (65 μM) or the storage buffer was added, with constant stirring, to the cuvette with the cell lysate. We excited the lysate with 433 nm and scanned the emission between 450 and 550 nm using a JASCO FP-6500 spectrofluorotometer. The instrument was programmed to record each spectrum three times and obtain the average; the difference between the individual spectras was less than 0.01% of the average. The values at the peaks corresponding to the maximum of CFP emission (490 nm) and YFP (525 nm) were logged in as "total CFP fluorescence" and "total YFP fluorescence", respectively. We monitored the changes in these values upon addition of GST-R7DEP, GST, or the storage buffer in which the GST or GST-R7DEP stocks were prepared. To study the dose dependence of this fluorescence change from added GST-R7DEP, the stock solution was consecutively added to the lysate in 50 μL increments. GST stock or the buffer was added in a similar manner to the control aliquots of the lysate. Upon addition of each portion of the GST-R7DEP or GST stock, the recorded fluorescence values dropped by approximately 2.5% due to the dilution of the lysate. To calculate the specific effect of GST-R7DEP, the CFP and YFP fluorescence values determined upon addition of GST (F_{GST}) were subtracted from the values obtained with GST-R7DEP (F_{DEP}). The difference is positive for CFP and negative for YFP. The difference between F_{GST} and F_{DEP} was proportional to the GST-R7DEP concentration. The effect of GST is identical to the effect of the buffer.

R7BP-Expressing Stable CHO-K1 Cells. A stable cell line expressing R7BP (CHO-R7BP) was generated through clonal selection on geneticin. Clones were analyzed by western blot, and six were selected and characterized with respect to recruitment of RGS7 to the membrane. The clone with the highest R7BP expression was used in the experiments.

Ca^{2+} Mobilization Assay. CHO-K1 or CHO-R7BP cells were transiently transfected, using a standard protocol (*21*), with cDNAs for M3 muscarinic receptor, RGS7 and Gβ_5, or Lac Z, as required by the experiment. Transfected cells were grown on coverslips and 48 h later were washed with 2% FBS in HBSS. Cells were the incubated in 2% FBS in HBSS containing 1 μM fura-2AM for 45 min at ambient temperature in the dark. This was followed by a 30 min incubation in Locke's buffer to permit the deesterification of fura-2AM. The coverslips were then secured in a flow chamber and mounted on the stage of a Nikon TE2000 inverted fluorescence microscope. The cells were continuously perfused with Locke's buffer and stimulated with 100 μM carbachol in the same buffer. The images were collected in real time every 2 s using a 20× UV objective lens and recorded using Metafluor software. The excitation wavelengths were 340 and 380 nm, and the emission was set at 510 nm. Free Ca^{2+} concentration was determined from the fluorescence measurements using the fura-2 Ca^{2+} imaging calibration kit (Molecular Probes) according to manufacturer's instructions.

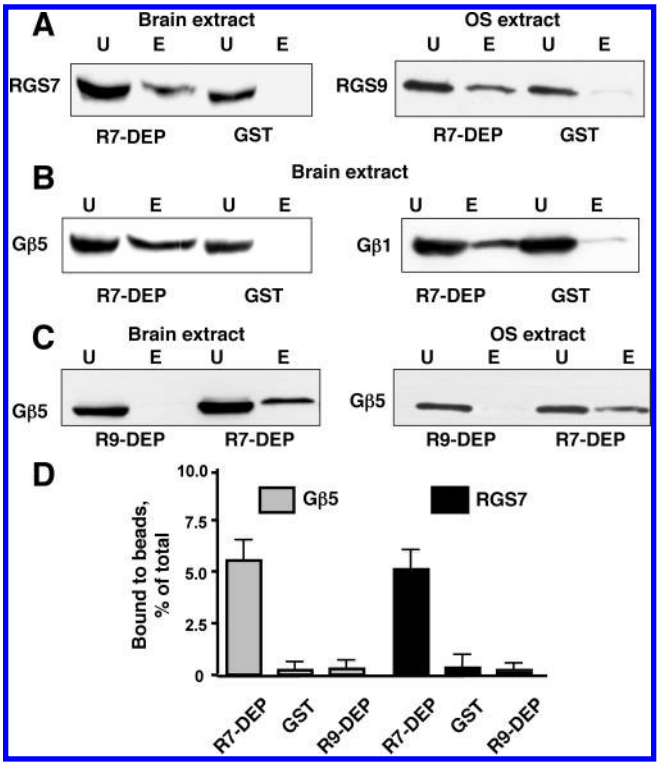

FIGURE 1: Interaction of the DEP domain of RGS7 with native Gβ_5-RGS complexes. GST fusions of the DEP domains of RGS7 or RGS9 (R7-DEP, R9-DEP) or GST were immobilized on glutathione−Sepharose beads. The beads were incubated batchwise with extracts from mouse brain or bovine photoreceptor outer segments (OS), as described in Materials and Methods. After the slurry was spun down and the unbound material was collected, the resin was washed and eluted with SDS−PAGE sample buffer. The unbound (U) and eluted (E) material was analyzed by western blot. (A) Mouse brain or bovine OS extracts were subjected to pull down with GST fusion of the RGS7 DEP domain, using GST as the negative control. The fractions from the pull-down assay were probed with the antibodies to RGS7 or RGS9, respectively. (B) Mouse brain extract was subjected to pull down, and the fractions were probed for the presence of Gβ subunits Gβ_5 and Gβ_1. (C) DEP domains of RGS7 and RGS9 were compared in their ability to bind Gβ_5 complexes in brain and OS extracts. (D) The amount of Gβ_5-RGS7 bound to the GST-R7DEP beads was determined as a fraction of total Gβ_5-RGS7 in the brain extract. Gels were scanned and analyzed with Scion software. To ensure that the amount of Gβ_5 loaded in the unbound and eluted lanes was within the linear range of the film and scanner, material in the eluate was 5 times more concentrated relative to the unbound (see Materials and Methods for details). Data show the mean ± standard deviation from eight independent experiments.

RESULTS

The Recombinant DEP Domain of RGS7 Binds to Native Gβ_5 and Gβ_1 Complexes. To identify the potential binding partners of the DEP domain of RGS7, we generated a GST fusion construct containing the amino acids 34−124 of bovine RGS7, termed GST-R7DEP or R7-DEP throughout this study. Using glutathione−Sepharose coupled to this GST fusion protein as an affinity matrix for the analysis of brain extracts, we unexpectedly found that it retained native RGS7-Gβ_5 complexes (Figure 1A,B). Similarly, GST-R7DEP bound to the Gβ_{5L}-RGS9 complex solubilized from the preparations of bovine photoreceptor outer segments (OS). The Gβ_5-RGS complexes from either source did not bind to the beads with GST or the GST fusion of the putative DEP domain of RGS9 (amino acids 20−117), indicating that the interaction of Gβ_5-

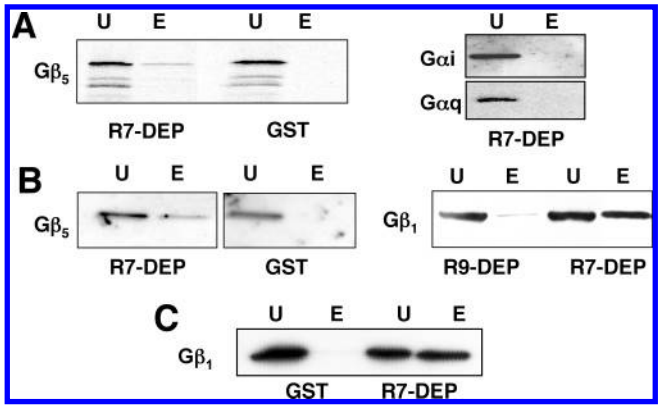

FIGURE 2: Interaction of the RGS7 DEP domain with recombinant $G\beta_5$ or $G\beta_1$. (A) $G\beta_5$ or the Gα subunits $G\alpha_i$ and $G\alpha_q$ were translated in vitro in the presence of [^{35}S]methionine and subjected to pull-down assay with the GST fusion of the RGS7 DEP domain (R7-DEP). The unbound (U) and eluted (E) material was resolved by SDS−PAGE, transferred to nitrocellulose, and detected by autoradiography. (B) Left panel: Western blot (anti-$G\beta_5$ antibody) of the unbound (U) and eluted (E) fractions from the GST-R7DEP pull down of the $G\beta_5\gamma_2$ complex transiently expressed in HEK 293 cells. Right panel: Pull down with the DEP domains of RGS7 and RGS9 of the transiently expressed $G\beta_1\gamma_2$ complex; the fractions were probed with anti-$G\beta_1$ antibody. (C) The homogeneous baculovirus-expressed $G\beta_1\gamma_2$ complex (2.5 μL of 1 mg/mL stock) was subjected to the pull down with GST-R7DEP, and the fractions were analyzed by western blot using anti-$G\beta_1$ antibody.

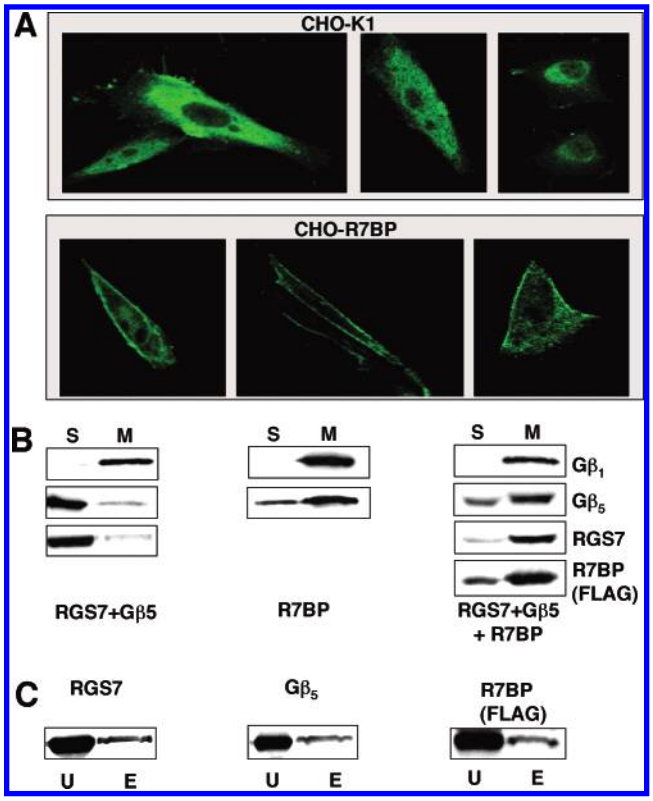

FIGURE 3: Effect of R7BP on the association of $G\beta_5$-RGS7 with cell membranes and GST-R7DEP. (A) YFP-RGS7 and $G\beta_5$ were transiently expressed in either control CHO-K1 cells or the CHO cell line stably expressing FLAG-tagged R7BP (CHO-R7BP). The cells were grown on glass coverslips, fixed, and visualized by laser confocal microscopy to detect YFP fluorescence. Shown are typical images from three independent transfection experiments. (B) CHO cells were lysed by hypotonic shock and freeze−thawing, and the lysate was centrifuged at 14000 rpm for 30 min to obtain membrane (M) and cytosolic (soluble, S) fractions. The soluble fraction was stored, and the pellet was resuspended in hypotonic buffer with 1% cholate. Lysate was vortexed vigorously and centrifuged at 14000 rpm for 20 min, and the supernatant was retained. These fractions were analyzed by western blot with antibodies against $G\beta_1$, $G\beta_5$, RGS7, and FLAG tag. (C) The membrane extract of the CHO-R7BP cells cotransfected with $G\beta_5$ and RGS7 was subjected to the pull down with GST-R7DEP, and the fractions were analyzed by western blot using antibodies against $G\beta_5$, RGS7, and FLAG tag.

RGS complexes with GST-R7DEP was specific. The eluates from GST-R7DEP beads did not contain any distinct proteins detectable by Coomassie or silver stain (data not shown). However, the antibody against $G\beta_1$ revealed its presence in the eluates from the GST-R7DEP beads (Figure 1B), suggesting that the DEP domain cannot distinguish between the $G\beta$ subunit subtypes.

GST-R7DEP Interacts with Recombinant $G\beta_5$ and $G\beta_1$. To determine which entities, $G\beta$, $G\gamma$, or RGS, are responsible for the interaction with the RGS7 DEP domain, we used GST-R7DEP for the pull-down of recombinant $G\beta_5$ and $G\beta_1$ subunit complexes. Figure 2A shows that in vitro translated $G\beta_5$ specifically bound to the beads with GST-R7DEP but not to the beads with GST. In contrast, other in vitro translated proteins, such as Gα subunits, $G\alpha_i$ or $G\alpha_q$, did not bind to GST-R7DEP under the same conditions. Similar to in vitro translated $G\beta_5$, $G\beta$ subunits type 1 or 5 transiently expressed in cultured COS-7 or HEK 293 cells also associated with the DEP domain of RGS7. Like their native counterparts (Figure 1), these recombinant $G\beta$ subunits did not bind to GST or the DEP domain of RGS9, supporting the specificity of the interaction with RGS7 DEP under these conditions. Importantly, the interaction of either $G\beta_1$ or $G\beta_5$ with GST-R7DEP was unaffected by the presence of $G\gamma$. Although we cannot rule out that (a fraction of) the $G\beta$ subunits were associated with endogenous $G\gamma$ subunits present in either the transfected cells or reticulocyte lysate, this observation indicated that the $G\beta$ is sufficient for interaction with the DEP domain. To rule out the potential contribution of any additional molecules present in the cellular extracts or reticulocyte lysate, we used a purified recombinant $G\beta_1\gamma_2$ complex (Figure 2C). We detected a robust interaction of this $G\beta\gamma$ complex with the RGS7 DEP domain. Taken together, these results indicate that the DEP domain of RGS7 can directly bind to G protein β subunits, apparently regardless of their subtype.

Effect of R7BP on Membrane Association of the $G\beta_5$-RGS7 Dimer and Its Interaction with R7-DEP. We investigated the effect of the recently discovered binding partner of the RGS7 DEP domain, R7BP, on the interaction between the DEP domain and $G\beta_5$; RGS7 and $G\beta_5$ (wild type or YFP fusion) were cotransfected with FLAG-tagged R7BP in either transiently transfected COS-7 (data not shown) or stably transfected R7BP-expressing CHO (CHO-R7BP) cells (Figure 3). Consistent with the original report (*42*), confocal microscopy showed that R7BP promoted localization of the RGS7 complex to the plasma membrane (Figure 3A). Noteworthy, tagging the N-terminus of RGS7 with YFP did not prevent the RGS7-R7BP interaction. Biochemical fractionation of cell lysates (Figure 3B) confirmed that R7BP partitioned primarily to the membrane. The endogenous $G\beta_1$, which we used as the membrane marker, was found only in the membrane pellet, showing that the cytosolic fraction was

free of residual membranes. There was a clear increase in the amount of RGS7 and Gβ_5 in the membrane fraction (Figure 3B) of CHO-R7BP compared to wild-type CHO (CHO-K1) cells. However, a portion of Gβ_5 and RGS7 was still found in the soluble fraction in the presence of R7BP, corroborating the presence of YFP fluorescence in the cytosol (Figure 3A). Next, we subjected the detergent extract from the membranes to the pull-down assay with GST-R7DEP (Figure 3C). Our results were similar to those obtained with the native tissues (Figure 1A,B). We also found that the GST-R7DEP pull down of Gβ_5-RGS7-R7BP was similar to the pull down of the Gβ_5-RGS7 dimer (Figure 4A). Therefore, we further investigated the DEP-Gβ_5 interaction using lysates of cells transfected with only two cDNAs, Gβ_5 and RGS7.

The Interaction between the RGS7 DEP Domain and Gβ_5 Is Dynamic. Our data on brain and OS extracts suggested that recombinant R7-DEP binds to the native Gβ_5-RGS complexes, which implied that the presence of the endogenous DEP domain could not completely prevent this interaction. One of the mechanisms allowing this interaction could be the competition of the exogenous GST-R7DEP with the endogenous DEP domain for the same site on Gβ_5. In this scenario, the deletion of the intrinsic DEP domain should enhance the association of R7-DEP with a DEP-less Gβ_5-RGS7 complex. To test this, we prepared two RGS7 constructs lacking the DEP domain: ΔDEP-RGS7, which lacks amino acids 34−125 (putative DEP domain), and RGS7$^{249-469}$, which lacks the first 248 amino acids encompassing the DEP domain along with the N-terminus and the linker region (Figure 4). These constructs were transiently expressed in COS-7 cells together with Gβ_5, and the resulting heterodimers were subjected to the pull-down assay using GST-R7DEP. Our data showed that both DEP-less constructs bound to GST-R7DEP much more efficiently than the full-length RGS7-Gβ_5 (Figure 4A). We explain the increased efficiency of the pull down as resulting from the lack of competition from the intrinsic DEP domain.

To confirm this conclusion, we used a reciprocal pull down, where the DEP domain was soluble and the Gβ_5-RGS complexes were immobilized via an antibody against the C-terminus of RGS7 (Figure 4C). In this alternative assay, we utilized the N-terminal portion of RGS7 encompassing the DEP domain and the linker region (amino acids 1−248) fused to the C-terminus of yellow fluorescent protein, YFP-R7$^{1-248}$. Fusion to YFP enabled detection of this construct using an anti-GFP antibody. YFP-R7$^{1-248}$ was cotransfected in COS-7 cells together with Gβ_5 and either full-length RGS7, ΔDEP, or RGS7$^{249-469}$. The cell lysates were immunoprecipitated with the antibody against the C-terminus of RGS7, and the fractions were probed for the presence of YFP-R7$^{1-248}$. We found that YFP-R7$^{1-248}$ was retained by the protein A beads with anti-RGS7 antibody, showing that the N-terminal portion of RGS7, apparently via the DEP domain, can physically associate with the Gβ_5-RGS7 dimers. Furthermore, co-immunoprecipitation tended to be more efficient with the DEP-less RGS7 constructs, supporting our data from the GST pull-down experiments (Figure 4A). Together, these results indicate that the exogenously added DEP domain competes with the intrinsic DEP domain present in full-length RGS7 for binding to Gβ_5.

To permit the association of the exogenously added DEP domain with Gβ_5, the intramolecular interaction between the intrinsic DEP and Gβ_5 must be dynamic, permitting the competition between the exogenous and endogenous DEP domains. To investigate this hypothesis, we devised a protein−protein binding assay based on fluorescence resonance energy transfer (FRET). The advantage of this

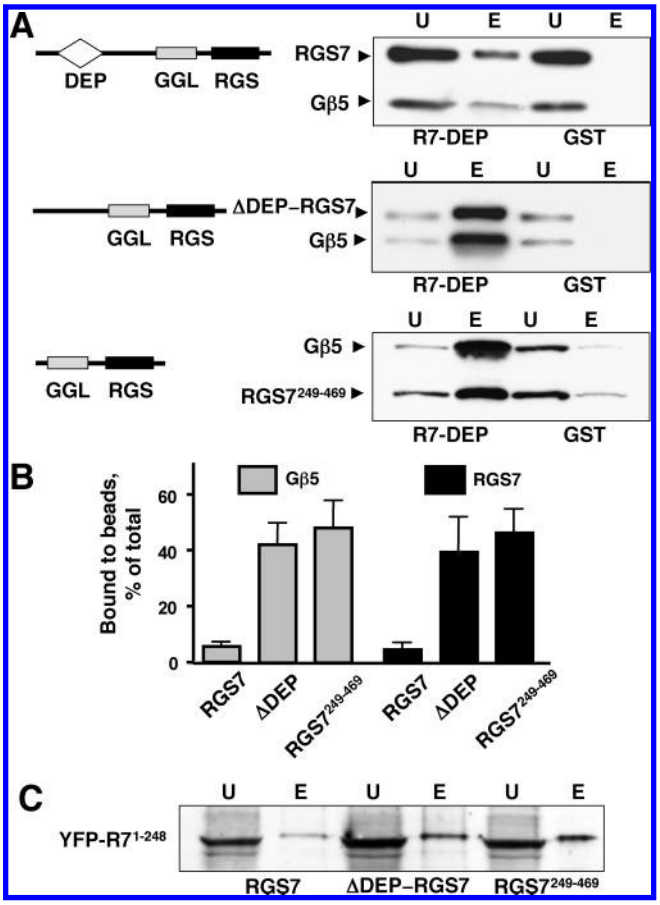

FIGURE 4: Endogenous DEP domain reduces the interaction of RGS7-Gβ_5 dimers with the recombinant RGS7 DEP. (A) COS-7 cells were transfected with full-length RGS7, ΔDEP-RGS7, and RGS7$^{249-469}$. The schematic drawings of these constructs depict the approximate location of the DEP (diamond), GGL (gray rectangle), and RGS (black rectangle) domains along the RGS7 polypeptide (black line). All of the constructs were cotransfected together with Gβ_5 cDNA to ensure their stability. Total cell lysates were prepared 48 h posttransfection and incubated with GST-R7DEP or GST bound to glutathione−Sepharose beads. Unbound (U) and eluted (E) fractions were analyzed by SDS−PAGE and detected after western blotting. The filters were first probed with the antibody against RGS7, developed, and subsequently probed with the antibody against Gβ_5. Since each antibody detected a single band and the antigens differed significantly in molecular weight, stripping of the blots between the probing with the two antibodies was not required. (B) The amount of the DEP-less Gβ_5-RGS7 constructs bound to the GST-R7DEP beads was compared to that of the full-length Gβ_5-RGS7. Gels were scanned and analyzed with Scion software as described in the legend to Figure 1D and in more detail in Materials and Methods. Data show the mean ± standard deviation from three (DEP-less constructs) and four (full-length RGS7) independent experiments. (C) As in (A), cells were transfected with either RGS7, ΔDEP-RGS7, or RGS7$^{249-469}$ constructs together with Gβ_5. In addition, the transfection mixture contained the plasmid encoding the fusion of yellow fluorescent protein (YFP) with the first 248 amino acids of RGS7, YFP-RGS7$^{1-248}$. Cell lysates prepared as in (A) were subjected to immunoprecipitation with an antibody against the C-terminus of RGS7 bound to protein A−Sepharose. The unbound (U) and eluted (E) fractions were analyzed by western blotting with anti-GFP antibody to detect the YFP-RGS7$^{1-248}$ fusion protein.

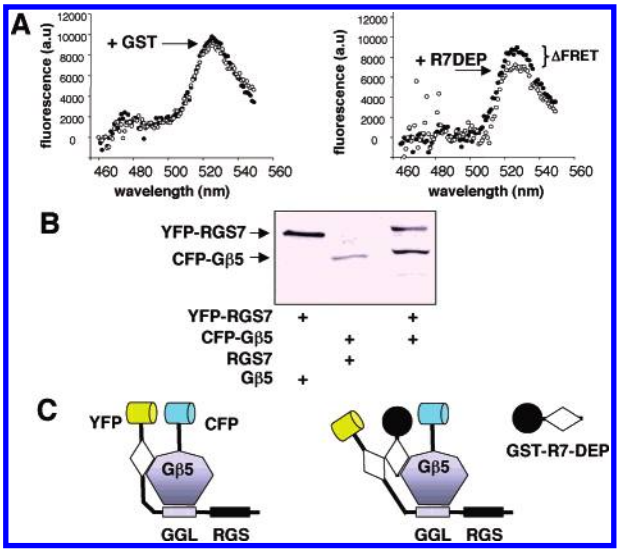

FIGURE 5: Fluorescence resonance energy transfer from CFP-Gβ5 to YFP-RGS7 is reduced by the GST fusion of the RGS7 DEP domain. To measure FRET, COS-7 cells were transiently transfected with plasmids encoding YFP-RGS7 and CFP-Gβ5. Control cells were cotransfected with YFP-RGS7 together with untagged Gβ5 and with CFP-Gβ5 together with untagged RGS7. The lysates of these cells were subjected to spectroscopic analysis, as described in Materials and Methods. Shown are the resulting FRET spectra obtained after subtraction of the YFP background fluorescence during the CFP excitation and CFP bleed-through into the YFP emission channel. (A) Right panel: GST-R7DEP (black symbols) or buffer (open symbols) was added to the lysate prior to recording of the spectra. Left panel: GST (black symbols) or buffer (white symbols) was added to an aliquot of the same lysate. (B) Western blot showing the expression of the fluorescent proteins in COS-7 lysate (15 μg of total protein) that was used in these experiments. (C) Our model: The drawing illustrates YFP fused to the N-terminus of RGS7 and CFP fused to the N-terminus of Gβ5, which form a strong FRET pair. This state represents the closed conformation of the Gβ5-RGS7 heterodimer. In the presence of GST-R7DEP fusion (black circle depicts GST), the intrinsic DEP domain cannot reassociate with Gβ5, but since the YFP fluorophore remains sufficiently close to the CFP tag, FRET can still occur, albeit to a lesser degree. This state represents the open conformation of the Gβ5-RGS7 molecule.

approach is that the interaction is detected in solution and does not require trapping of the protein complex on a solid phase and the required washes. In FRET, the energy from the photoexcited fluorophore ("donor") is transferred to the acceptor fluorophore without emission, and the acceptor then emits this energy at the longer wavelength. Since energy transfer efficiency drops exponentially as the distance between the fluorophores increases, FRET can be used to study the physical interaction between a pair of fluorescently tagged molecules. We employed the previously characterized (*21*, *45*) CFP-Gβ5 and YFP-RGS7 fusions as the FRET energy donor and acceptor, respectively. No FRET was registered between CFP-Gβ5 and YFP or YFP-RGS7 constructs and CFP (data not shown).

We reasoned that if the exogenously added GST-R7DEP can compete with the intrinsic DEP domain in the pull-down assay (Figure 4), one could expect it to do so in solution. The dissociation between the intrinsic Gβ5 and DEP domain within the Gβ5-RGS7 dimer might increase the distance between CFP and YFP tags, leading to a possible reduction in FRET. This was exactly what we observed: GST-R7DEP, but not GST alone, decreased FRET (Figure 5A), pointing to the dynamic nature of the DEP-Gβ5 association within the Gβ5-RGS dimer. The FRET reduction did not exceed 15−20% of the total FRET signal.

Measuring FRET requires subtraction of CFP fluorescence in the YFP emission channel ("bleed-through") and of YFP background fluorescence from the spectra obtained from samples containing both CFP-Gβ5 and YFP-RGS7. Therefore, additional spectra must be recorded from control cells expressing only CFP-tagged and only YFP-tagged molecules. The inherent variability of protein expression in transient transfection made the calculations of FRET and comparison of different experiments difficult. To circumvent these technical problems, we used a simplified method based on the measurements of changes in *total* fluorescence in the same COS-7 cell lysate, which contained full-length YFP-RGS7 and CFP-Gβ5 (Figure 6). In this approach, the background (nonspecific fluorescence of the cell lysate, CFP bleed-through to the YFP channel, and the emission of 433 nm excited YFP) was not subtracted from the recorded measurements, and so the bona fide FRET could not be determined. However, there is no variability in this background because the measurements are performed on the same lysate preparation. The very low "noise" in this method allowed us to reliably detect the specific effect of GST-R7DEP on fluorescence of the CFP-Gβ5/YFP-RGS7 complex. For this purpose, we compared the changes in total YFP and CFP fluorescence upon addition of the increasing amounts of GST-R7DEP or GST (F_{DEP} and F_{GST}, respectively). Consecutive additions of GST-R7DEP or GST resulted in incremental dilutions of the lysate and corresponding reduction of total fluorescence (Figure 6A,B). The reduction detected in the presence of GST was identical to that caused by addition of the buffer in which GST or GST-R7DEP was prepared. This confirmed that, for both YFP and CFP, the reduction of F_{GST} represented the dilution-dependent drift of the baseline. The addition of GST-R7DEP elicited a stronger reduction of YFP fluorescence compared to GST: $F_{DEP} < F_{GST} = F_{buffer}$ (Figure 6A). The difference between F_{GST} and F_{DEP} is very small compared to the total fluorescence, but it can be reliably detected because we use identical aliquots of the same lysate for these measurements. We think that the value of F_{DEP} is lower than the value of F_{GST} because of the reduction in the amount of energy YFP-RGS7 receives from CFP-Gβ5. Importantly, the effect of GST-R7DEP on fluorescence of the donor fluorophore, CFP-Gβ5, was opposite to its effect on YFP: $F_{DEP} > F_{GST} = F_{buffer}$ (Figure 6B). The fact that the donor fluorescence increases concurrently with the decrease of the acceptor fluorescence strongly indicates that GST-R7DEP attenuates FRET between CFP-Gβ5 and YFP-RGS7 (Figure 6C). The fact that the absolute value of drop in YFP fluorescence is higher than the increase in CFP fluorescence is consistent with the fact that YFP is a brighter emitter than CFP. The GST-R7DEP-mediated FRET reduction was dose-dependent within the range of concentrations of GST-R7DEP that we were able to achieve (up to 10^{-5} M). The simplest interpretation of these results is the competition of GST-R7DEP with the endogenous DEP domain for the binding site on Gβ5.

The Putative Binding Site for Gβ5 on the RGS7 DEP Domain. An important step in the characterization of a protein−protein interaction is the identification of the binding site through generation of interaction-deficient mutants. The design of an RGS7 DEP mutant incapable of Gβ5 binding

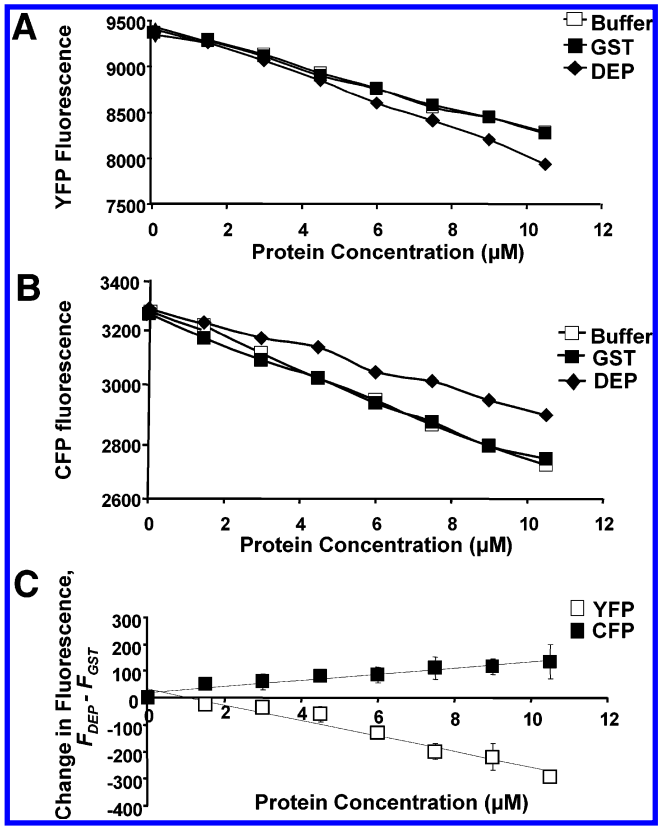

FIGURE 6: Dose-dependent effect of GST-R7DEP on the CFP-Gβ_5/YFP-RGS7 dimer. COS-7 cells were transiently transfected with YFP fusion of full-length RGS7 (YFP-RGS7) and CFP-Gβ_5. Three 2 mL aliquots of the cell lysate were analyzed using a fluorescence spectrophotometer. To one portion of the lysate was added purified GST-R7DEP (black diamonds), another aliquot was mixed with GST (black squares), and the third aliquot was mixed with buffer (white squares). The protein stocks (65 μM) or buffer was added to the quartz cuvette in 50 μL increments with continuous stirring. After each addition, total fluorescence values at the YFP maximum (525 nm, shown in panel A) and CFP maximum (490 nm, panel B) were determined; the excitation wavelength was set at 433 nm, and the spectra were taken as described in Materials and Methods. (A) Raw data showing a single representative experiment where 525 nm fluorescence is plotted against the concentration of GST or GST-R7DEP in the mixture. Note that the *Y* axis starts with 7500 arbitrary fluorescence units, and the specific effect of GST-R7DEP is small. However, it is clearly discernible compared to the effect of lysate dilution, which is seen as the stable decline of the signal in the presence of buffer or GST. (B) Total 490 nm (CFP emission maximum) fluorescence recorded in the same experiment; raw data. (C) Summary of data from four independent experiments (independent COS-7 cell transfections). *Y* axis: Data show the difference between fluorescence recorded in the presence of GST-R7DEP (F_{DEP}) and fluorescence measured in the presence of GST (F_{GST}), $F_{DEP} - F_{GST}$ (mean ± standard deviation). Black symbols designate YFP fluorescence; white, CFP. Note that the $F_{DEP} - F_{GST}$ difference is negative for YFP and positive for CFP. The lines connecting the values represent a linear regression fit of the data ($r^2 > 0.94$ for both YFP and CFP).

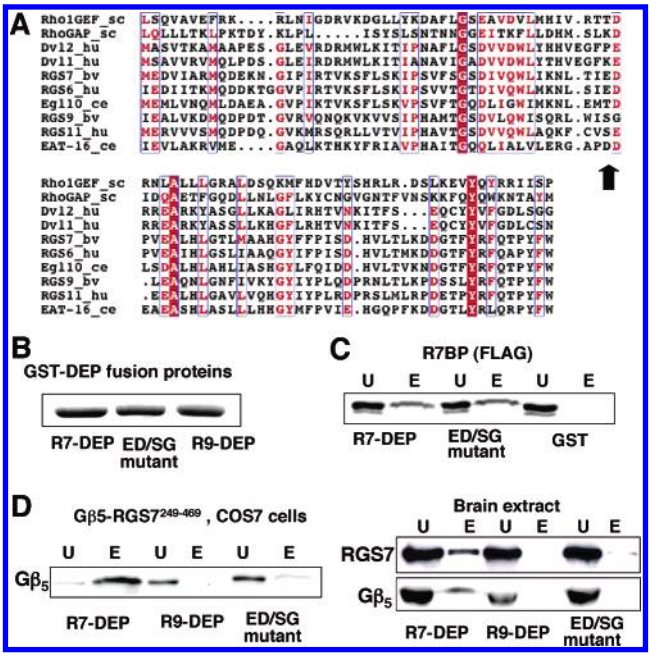

FIGURE 7: Potential Gβ_5 binding site on RGS7 DEP. (A) Amino acid sequence alignment of putative DEP domains of R7 RGS proteins. Multiple sequence alignment was generated by MAFFT using an iterative refinement method and JTT200 scoring matrix (*61*, *62*) and ESPript 2.2 (*63*). Identical residues are shaded in red. Conserved blocks of amino acids are represented as blue boxes. Abbreviations: hu, human; bv, bovine; ce, *C. elegans*; sc, *Saccharomyces cerevisiae*. The arrow indicates the position of the two acidic residues, Glu73 and Asp74, of RGS7 that were mutated. (B) Commassie-stained gel illustrating the purity of the GST fusion proteins: GST-R7DEP, GST-R9DEP, and the mutant of GST-R7DEP (ED/SG), where amino acids Glu73 and Asp74 in RGS7 were substituted by Ser and Gly, respectively. Equal amounts of these proteins were loaded on the glutathione beads in the subsequent pull-down assays. (C) The ED/SG mutant was tested for its ability to bind transiently expressed R7BP (FLAG antibody). (D) Left panel: Representative experiment where the Gβ_5-RGS7$^{249-469}$ complex was transiently expressed in COS-7 cells and subjected to the pull down with the indicated GST fusion proteins. The unbound (U) and eluted (E) fractions were analyzed by western blot with the Gβ_5 antibody. Right panels: Mouse brain extract was subjected to the pull down, and the fractions were probed with either anti-RGS7 or anti-Gβ_5 antibodies.

was aided by our finding that the DEP domain of RGS9 does not bind to Gβ_5. The alignment of DEP domains revealed that the most striking difference in the distribution of charged amino acids was the absence in RGS9 of the negative charge at the position corresponding to Asp-74 in RGS7 (Figure 7A). A negatively charged amino acid is present at this position in all R7 RGSs except RGS9 and even in the DEP domains of Dishevelled, Rho1GEF, and RhoGAP. We hypothesized that the negative charge is important for the interaction with Gβ_5 and replaced Glu-73 and Asp-74 of RGS7 with Ser and Gly residues, which are present at the corresponding positions in the DEP domain of RGS9. This ED/SG mutant was expressed as a GST fusion in *E. coli* and utilized in pull-down assays. The purity of the recombinant ED/SG mutant, GST-R7DEP, and GST-R9DEP was confirmed by SDS−PAGE (Figure 7B). Extracts of mouse brain and COS-7 cells expressing Gβ_5 associated with RGS7 and RGS7$^{249-469}$ were subjected to the pull down (Figure 7D). These experiments showed that there was at least a 10-fold reduction in the amount of Gβ_5 that was pulled down by the ED/SG mutant relative to the wild-type DEP domain of RGS7. The ED/SG mutant, however, retained the ability to bind R7BP (Figure 7C), which showed that the overall folding of the DEP domain was not compromised by the mutation and that R7BP and the Gβ subunits likely associate with two distinct surfaces of the DEP domain.

The Effect of the E73S/D74G Double Mutation (ED/SG) on the Function of the Gβ_5-RGS7-R7BP Complex. Previous studies showed that the Gβ_5-RGS7 complex can attenuate G_q-mediated Ca^{2+} response to muscarinic M3 receptor

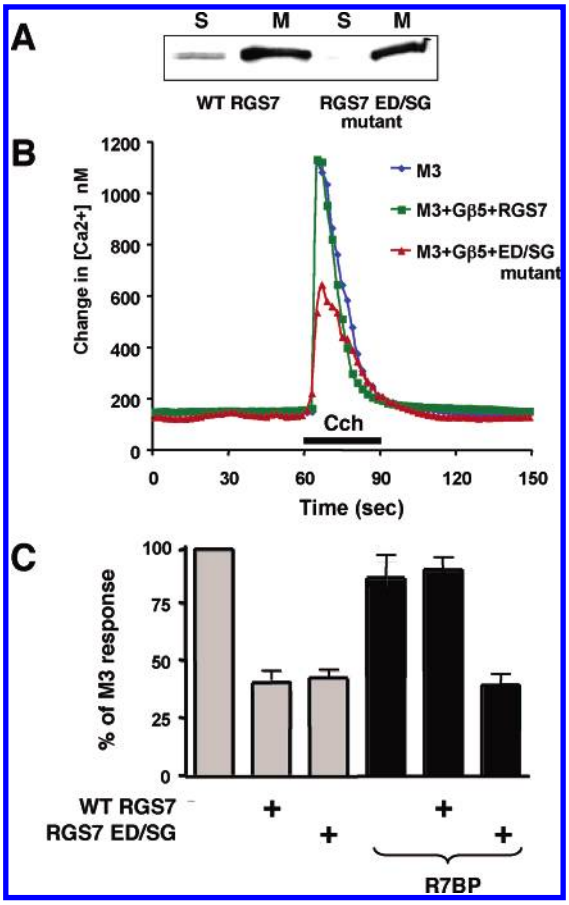

FIGURE 8: Effect of the ED/SG mutation and R7BP on the function of the $G\beta_5$-RGS7 complex. The double mutation E73S/D74G was introduced into the full-length RGS7 in the pcDNA3 plasmid. The $RGS7^{ED/SG}$ mutant was transiently transfected, along with $G\beta_5$ and muscarinic M3 receptor cDNAs into wild-type CHO-K1 and CHO-R7BP cells. (A) Western blot analysis showing the similar distribution of the wild-type RGS7 and $RGS7^{ED/SG}$ mutant between the membrane and cytosolic fractions of CHO-R7BP cells. (B) Carbachol-induced Ca^{2+} transients in CHO-R7BP cells. Cells were transfected with M3 receptor, $G\beta_5$, and either wild-type RGS7 or the $RGS7^{ED/SG}$ mutant. Cells were plated on glass coverslips and loaded with fura-2, and fluorescence was recorded in real time as described in Materials and Methods. The application of 100 μM carbachol (Cch) is denoted with the black bar. Shown are representative traces from single cells. (C) The mean amplitude ± SD of the Ca^{2+} responses from five independent experiments. In each experiment, traces were recorded from 20 randomly selected carbachol-responding cells. The determined average response was expressed as the percent value compared to the average response of cells transfected only with M3 receptor (in the absence of RGS7, $G\beta_5$, and R7BP), which was set as 100% response. Black bars represent CHO-R7BP cells. Gray bars represent CHO-K1 cells.

stimulation in transfected cells (*20*, *21*). Here, we used this assay to study the effect of the ED/SG mutation on the function of full-length RGS7 protein (Figure 8). The $RGS7^{ED/SG}$ mutant was transiently expressed together with $G\beta_5$ and the M3 receptor in CHO-K1 cells. To test the role of R7BP, we used the CHO cell line stably expressing R7BP, CHO-R7BP. The rationale behind using the stable R7BP transfection was to limit the number of transiently transfected cDNAs to three. Western blot analysis showed that, similar to the wild-type RGS7, the $RGS7^{ED/SG}$ mutant was localized to the membranes in the presence of R7BP, showing that the ED/SG mutation did not affect the R7BP interaction with the $G\beta_5$-RGS7 dimer (Figure 8A). We then recorded the changes in free Ca^{2+} concentration in response to carbachol using the ratiometric dye, fura-2, in control CHO-K1 (data not shown) and in the CHO-R7BP cells (Figure 8B). The results of these recordings (Figure 8C) revealed two novel effects. First, we found that R7BP prevented Gβ5-RGS7 from exerting its negative effect on the carbachol-induced calcium mobilization. This negative effect of R7BP on Gβ5-RGS7 in this G_q-mediated pathway contrasts with its positive effect on Gβ5-RGS7 reconstituted with the G_i and GIRK channel in *Xenopus* oocytes (*42*). Second, we observed a dramatic difference between the wild type and $RGS7^{ED/SG}$ mutant (Figure 8C, black bars) in their ability to reduce the amplitude of Ca^{2+} response in the presence of R7BP. In the absence of R7BP, the mutant and wild-type RGS7 complexes inhibited Ca^{2+} responses to a similar degree (Figure 8C, gray bars). These results indicate that the inhibition of M3 receptor signaling by the $G\beta_5$-RGS7-R7BP complex occurs more efficiently when the interaction between the DEP domain and $G\beta_5$ is reduced.

DISCUSSION

G protein β subunits exist as obligatory heterodimers with Gγ subunits or, in the case of $G\beta_5$, with Gγ-like (GGL) domains of the R7 subfamily of RGS proteins. A hallmark feature of G$\beta\gamma$ complexes is their ability to interact with a large array of structurally diverse binding partners: Gα subunits, receptors, effectors, phosducins, etc. (for reviews, see refs *46*−*49*). The key finding of this study is the novel interaction involving Gβ subunits, an interaction with the DEP domain of RGS7.

Specificity of the DEP Domain-Gβ Interaction. We discovered the interaction of the DEP domain of RGS7 with Gβ subunits through the utilization of a GST pull-down assay (Figures 1 and 2). The results of this experiment met the basic criteria of binding specificity, such as the lack of Gβ retention on the beads with immobilized GST and the lack of association of GST-R7DEP fusion with the bulk of the proteins in the cellular lysates and with key molecules such as Gα subunits. The specificity of the GST-R7DEP pull down with $G\beta_5$ was corroborated by alternative assays such as immunoprecipitation (Figure 4C) and FRET (Figures 5 and 6).

Despite the reasonably high homology between the DEP domains of RGS7 and RGS9, the GST fusion of the RGS9 DEP domain did not bind to Gβ subunits under the same conditions (Figure 1C). This finding supported the specificity of the R7-DEP interaction with Gβ subunits even further and provided us with the strategy to determine the structural basis of the interaction. We focused on a particular conserved aspartic acid, D74 in RGS7, because it was present in all R7 RGS proteins and even in other proteins such as RhoGAP and Dishevelled but is replaced with a serine residue in RGS9. In RGS7, as well as RGS6, Egl-10, and Eat 16, this conserved Asp is adjacent to a Glu residue, presumably creating a significant negative charge. The substitution of these two amino acids, Glu and Asp, with the corresponding amino acids in RGS9 (Ser and Gly) was sufficient to diminish the DEP-$G\beta_5$ interaction, strongly indicating that the negative charge is essential for binding $G\beta_5$ (Figure 7C). Importantly, this mutation did not affect binding of the DEP domain to R7BP, indicating that the overall structure of the molecule remained intact. We cannot yet conclude that E73/

D74 of RGS7 constitutes the bona fide binding site for Gβ_5. However, considering the location of these residues in the currently available NMR structure for a similar DEP domain (*37*), this appears to be a reasonable prediction.

Since the monomeric Gβ_5 subunit can bind to GST-R7DEP (Figure 2), the binding site for the DEP domain is likely to be present on the Gβ chain rather than within the GGL domain. Since Gβ_1 and Gβ_5 subunits were similar in their binding to the RGS7 DEP domain, it is likely that the binding site is located in a conserved region of Gβ. Further structural studies will be required to find out if there are additional binding sites for the DEP domain within other parts of the RGS7 molecule.

The fusion of the DEP- and GGL-encoding genes, which evidently occurred during the evolution, caused Gβ_5 to be permanently tethered to the DEP domain via the linker region. In this study we focused on the hypothesis that this Gβ-R7DEP interaction represents the intramolecular association between the Gβ_5 subunit and the DEP domain. Indeed, it appears that, unless an additional mechanism can reduce the DEP-Gβ_5 binding affinity, the interaction between the intrinsic entities would be favored over the interaction with a competing free G$\beta\gamma$. However, at this point we do not rule out that the DEP domain of RGS7 or other DEP domains can interact with canonical G$\beta\gamma$ subunit complexes originating from the activated G proteins.

Possible "Open" and "Closed" Conformations of the Gβ_5-RGS7 Complex. Canonical Gβ subunits (types 1−4) are involved in two kinds of protein−protein interactions: the permanent association with Gγ and dynamic interactions involving G$\beta\gamma$ subunits. The association with the cognate Gγ subunits occurs cotranslationally and is essential for stability of both Gβ and Gγ molecules (*50*−*52*). According to the crystal structures of G$\beta\gamma$ dimers, there are numerous points of direct contact between the β and γ chains, and accordingly, they dissociate only under denaturing conditions. Compared to the Gβ-Gγ association, interactions of G$\beta\gamma$ complexes with Gα, effectors, and other binding partners have a relatively low affinity, and they are dynamically regulated by the signaling events in the G protein pathway.

Gβ_5 is permanently associated with GGL domains, which is crucial for the stability of the Gβ_5 and RGS subunits. Several studies have shown that, in vitro, Gβ_5 can associate with Gγ, and these Gβ_5-Gγ complexes can interact with Gα subunits and effectors (*25*, *53*, *54*). Although available evidence argues against the existence of Gβ_5-Gγ complexes in vivo, these experiments indicated that, like other Gβ subunits, Gβ_5 is able to participate in dynamic interactions with other signaling proteins. However, physiologically relevant binding partners of the Gβ_5-GGL module of the Gβ_5-RGS dimers have not been found. In this paper, we have identified the DEP domain of RGS7 as a binding partner of Gβ_5. The pull down of the full-length RGS7-Gβ_5 complex by GST-R7DEP (Figures 1−3), the enhanced binding of the DEP-less RGS7 constructs (Figure 4), and FRET (Figures 5 and 6) all indicate that the endogenous DEP domain can be displaced from Gβ_5/GGL. We think that these results can be best explained by the following model: in contrast to the permanent Gβ5-GGL interaction, the interaction between Gβ_5 and the DEP domain is dynamic in nature, and the Gβ_5-RGS7 complex can exist in (at least) two distinct conformations, open, when the DEP domain does not make contact with Gβ_5, and closed, when the DEP domain is in physical contact with Gβ_5.

Importantly, the fact that native Gβ_5-RGS7 and Gβ_5-RGS9 complexes do interact with GST-R7DEP indicates that the open conformation exists in situ. According to the estimates based on the quantification of the pull-down data, this fraction does not exceed 5−10% of the total Gβ_5-RGS7 amount (Figure 1D). However, because this pool appears to represent the "active" state of the RGS7 complex, it is likely to be significant. Supporting the idea that the RGS7 complex can exist in more than one form, Hepler and colleagues found that brain membrane RGS7 could be separated into two pools distinct in detergent solubility (*55*). It is tempting to speculate that the distinct native pools of the Gβ_5-RGS7 complex, identified by the Hepler group and in our current study, may participate in different signaling pathways, depending on the localization and the conformational state of the complex.

Potential Role of the Gβ_5-DEP Interaction. To explore the significance of the DEP-Gβ_5 interaction, we mutated the putative Gβ_5 binding site on the RGS7 DEP domain and tested the functional activities of the resulting Gβ_5-RGS7 and Gβ_5-RGS7-R7BP complexes (Figure 8). Our results showed that, like wild-type RGS7, the RGS7$^{ED/SG}$ mutant attenuated M3 receptor-induced Ca^{2+} mobilization. However, the mutant retained its activity in the presence of R7BP, whereas R7BP abolished the activity of the wild-type RGS7. This allowed us to infer that when Gβ_5 and DEP are dissociated, Gβ_5-RGS7 is more active with respect to inhibition of G_q-mediated signaling. When Gβ_5 and DEP domains interact, the molecule assumes the closed conformation, which is less active toward G_q-mediated signaling. Testing this hypothesis will require further investigation.

In addition to the regulation of RGS7-mediated effects on G protein signaling, the DEP-Gβ_5 interaction may play other role(s). It was previously found that the N- and C-terminal fragments of Egl-10, a *C. elegans* orthologue of RGS7, complemented each other in mimicking the functional activity of Egl-10 (*56*). Egl-10 negatively regulates G_o-mediated signaling in the worm, whereas a similar RGS protein, Eat-16, regulates the G_q-mediated pathway. The severed C-terminal portion of Egl-10 could regulate either G_o- or G_q-mediated signaling. Thus, the N-terminus of Egl-10 determines the selectivity of the RGS complex to the specific G protein pathway. The direct interaction between the DEP domain and Gβ_5 identified in our current study may explain the complementation results in *C. elegans*. It is reasonable to expect that in mammals the DEP-Gβ_5 interaction also contributes to the specificity of receptor−effector coupling. Another possibility is that the DEP-Gβ_5 interaction plays a role in other intriguing phenomena whose significance is currently not understood: the nuclear localization of Gβ_5-RGS7 (*42*, *57*, *58*) and the potential relationship between Gβ_5-R7 and SNARE complex (*43*). Since Gβ_5 localizes to the nucleus when reconstituted with RGS7 but not Gγ (*58*), it is possible that the Gβ_5-DEP, rather than the Gβ_5-GGL, interaction is essential for nuclear targeting. The recently discovered interaction of G$\beta\gamma$ with SNARE complexes (*59*, *60*) hints at the influence that Gβ_5 may have on the interaction of DEP with snapin or R7BP, which itself slightly resembles SNARE proteins (*42*). Such an effect of Gβ_5 could play a role in neuronal vesicular trafficking and fusion.

The intradomain interaction identified in this study highlights the apparent advantage of modular molecules such as the R7 family of RGSs. Compared to diffusion, which may limit the rate of interactions involving simpler molecules like RGS4, the multidomain architecture permits coordination and acceleration of signaling events. Experiments presented in this paper show that, not unlike the G proteins themselves, the $G\beta_5$-R7 complexes may be "breathing" molecules, which undergo conformational changes that alter their functional activity.

ACKNOWLEDGMENT

We thank Rik Meyers and James Potter (University of Miami) for providing access to spectrophotometers and for helpful discussions concerning FRET. We are particularly grateful to Steve Roper (University of Miami) for invaluable help with Ca^{2+} imaging. We thank Carmen Dessauer (University of Texas, Houston) for providing the purified $G\beta\gamma$ complex and Ken Blumer (Washington University) for the R7BP construct.

REFERENCES

1. Siderovski, D. P., Strockbine, B., and Behe, C. I. (1999) Whither goest the RGS proteins?, *Crit. Rev. Biochem. Mol. Biol. 34*, 215.
2. Hepler, J. R. (1999) Emerging roles for RGS proteins in cell signalling, *Trends Pharmacol. Sci. 20*, 376.
3. Berman, D. M., and Gilman, A. G. (1998) Mammalian RGS proteins: barbarians at the gate, *J. Biol. Chem. 273*, 1269.
4. Burchett, S. A. (1998) Regulators of G protein signaling: a bestiary of modular protein binding domains, *J. Neurochem. 75*, 1335.
5. Abramow-Newerly, M., Roy, A. A., Nunn, C., and Chidiac, P. (2006) RGS proteins have a signalling complex: interactions between RGS proteins and GPCRs, effectors, and auxiliary proteins, *Cell. Signalling 18*, 579.
6. Khawaja, X. Z., Liang, J. J., Saugstad, J. A., Jones, P. G., Harnish, S., Conn, P. J., and Cockett, M. I. (1999) Immunohistochemical distribution of RGS7 protein and cellular selectivity in colocalizing with Galphaq proteins in the adult rat brain, *J. Neurochem. 72*, 174.
7. Elmore, T., Rodriguez, A., and Smith, D. P. (1998) dRGS7 encodes a *Drosophila* homolog of EGL-10 and vertebrate RGS7, *DNA Cell Biol. 17*, 983.
8. Gold, S. J., Ni, Y. G., Dohlman, H. G., and Nestler, E. J. (1997) Regulators of G-protein signaling (RGS) proteins: region-specific expression of nine subtypes in rat brain, *J. Neurosci. 17*, 8024.
9. Cowan, C. W., Fariss, R. N., Sokal, I., Palczewski, K., and Wensel, T. G. (1998) High expression levels in cones of RGS9, the predominant GTPase accelerating protein of rods, *Proc. Natl. Acad. Sci. U.S.A. 95*, 5351.
10. Cowan, C. W., He, W., and Wensel, T. G. (2001) RGS proteins: lessons from the RGS9 subfamily, *Prog. Nucleic Acid Res. Mol. Biol. 65*, 341.
11. He, W., Cowan, C. W., and Wensel, T. G. (1998) RGS9, a GTPase accelerator for phototransduction, *Neuron 20*, 95.
12. Lyubarsky, A. L., Naarendorp, F., Zhang, X., Wensel, T., Simon, M. I., and Pugh, E. N., Jr. (2001) RGS9-1 is required for normal inactivation of mouse cone phototransduction, *Mol. Vision 7*, 71.
13. Makino, E. R., Handy, J. W., Li, T., and Arshavsky, V. Y. (1999) The GTPase activating factor for transducin in rod photoreceptors is the complex between RGS9 and type 5 G protein beta subunit, *Proc. Natl. Acad. Sci. U.S.A. 96*, 1947.
14. Rahman, Z., Schwarz, J., Gold, S. J., Zachariou, V., Wein, M. N., Choi, K. H., Kovoor, A., Chen, C. K., DiLeone, R. J., Schwarz, S. C., Selley, D. E., Sim-Selley, L. J., Barrot, M., Luedtke, R. R., Self, D., Neve, R. L., Lester, H. A., Simon, M. I., and Nestler, E. J. (2003) RGS9 modulates dopamine signaling in the basal ganglia, *Neuron 38*, 941.
15. Kovoor, A., Seyffarth, P., Ebert, J., Barghshoon, S., Chen, C. K., Schwarz, S., Axelrod, J. D., Cheyette, B. N., Simon, M. I., Lester, H. A., and Schwarz, J. (2005) D2 dopamine receptors colocalize regulator of G-protein signaling 9-2 (RGS9-2) via the RGS9 DEP domain, and RGS9 knock-out mice develop dyskinesias associated with dopamine pathways, *J. Neurosci. 25*, 2157.
16. Posner, B. A., Gilman, A. G., and Harris, B. A. (1999) Regulators of G protein signaling 6 and 7. Purification of complexes with gbeta5 and assessment of their effects on G protein-mediated signaling pathways, *J. Biol. Chem. 274*, 31087.
17. Hooks, S. B., Waldo, G. L., Corbitt, J., Bodor, E. T., Krumins, A. M., and Harden, T. K. (2003) RGS6, RGS7, RGS9, and RGS11 stimulate GTPase activity of Gi family G-proteins with differential selectivity and maximal activity, *J. Biol. Chem. 278*, 10087.
18. Shuey, D. J., Betty, M., Jones, P. G., Khawaja, X. Z., and Cockett, M. I. (1998) RGS7 attenuates signal transduction through the G(alpha q) family of heterotrimeric G proteins in mammalian cells, *J. Neurochem. 70*, 1964.
19. DiBello, P. R., Garrison, T. R., Apanovitch, D. M., Hoffman, G., Shuey, D. J., Mason, K., Cockett, M. I., and Dohlman, H. G. (1998) Selective uncoupling of RGS action by a single point mutation in the G protein alpha-subunit, *J. Biol. Chem. 273*, 5780.
20. Witherow, D. S., Wang, Q., Levay, K., Cabrera, J. L., Chen, J., Willars, G. B., and Slepak, V. Z. (2000) Complexes of the G protein subunit gbeta 5 with the regulators of G protein signaling RGS7 and RGS9. Characterization in native tissues and in transfected cells, *J. Biol. Chem. 275*, 24872.
21. Witherow, D. S., Tovey, S. C., Wang, Q., Willars, G. B., and Slepak, V. Z. (2003) G beta 5. RGS7 inhibits G alpha q-mediated signaling via a direct protein-protein interaction, *J. Biol. Chem. 278*, 21307.
22. Hajdu-Cronin, Y. M., Chen, W. J., Patikoglou, G., Koelle, M. R., and Sternberg, P. W. (1999) Antagonism between G(o)alpha and G(q)alpha in *Caenorhabditis elegans*: the RGS protein EAT-16 is necessary for G(o)alpha signaling and regulates G(q)alpha activity, *Genes Dev. 13*, 1780.
23. Cabrera, J. L., de Freitas, F., Satpaev, D. K., and Slepak, V. Z. (1998) Identification of the Gbeta5-RGS7 protein complex in the retina, *Biochem. Biophys. Res. Commun. 249*, 898.
24. Zhang, J. H., and Simonds, W. F. (2000) Copurification of brain G-protein beta5 with RGS6 and RGS7, *J. Neurosci. 20*, RC59.
25. Watson, A. J., Katz, A., and Simon, M. I. (1994) A fifth member of the mammalian G-protein beta-subunit family. Expression in brain and activation of the beta 2 isotype of phospholipase C, *J. Biol. Chem. 269*, 22150.
26. Liang, J. J., Cockett, M., and Khawaja, X. Z. (1998) Immunohistochemical localization of G protein beta1, beta2, beta3, beta4, beta5, and gamma3 subunits in the adult rat brain, *J. Neurochem. 71*, 345.
27. Witherow, D. S., and Slepak, V. Z. (2003) A novel kind of G protein heterodimer: The Gbeta5-RGS complex, *Recept. Channels 9*, 205.
28. Snow, B. E., Krumins, A. M., Brothers, G. M., Lee, S. F., Wall, M. A., Chung, S., Mangion, J., Arya, S., Gilman, A. G., and Siderovski, D. P. (1998) A G protein gamma subunit-like domain shared between RGS11 and other RGS proteins specifies binding to Gbeta5 subunits, *Proc. Natl. Acad. Sci. U.S.A. 95*, 13307.
29. Levay, K., Cabrera, J. L., Satpaev, D. K., and Slepak, V. Z. (1999) Gbeta5 prevents the RGS7-Galphao interaction through binding to a distinct Ggamma-like domain found in RGS7 and other RGS proteins, *Proc. Natl. Acad. Sci. U.S.A. 96*, 2503.
30. Snow, B. E., Betts, L., Mangion, J., Sondek, J., and Siderovski, D. P. (1999) Fidelity of G protein beta-subunit association by the G protein gamma-subunit-like domains of RGS6, RGS7, and RGS11, *Proc. Natl. Acad. Sci. U.S.A. 96*, 6489.
31. Sondek, J., and Siderovski, D. P. (2001) Ggamma-like (GGL) domains: new frontiers in G-protein signaling and beta-propeller scaffolding, *Biochem. Pharmacol. 61*, 1329.
32. Jones, M. B., Siderovski, D. P., and Hooks, S. B. (2004) The G{beta}{gamma} dimer as a novel source of selectivity in G-protein signaling: GGL-ing at convention, *Mol. Interventions 4*, 200.
33. Chen, C. K., Burns, M. E., He, W., Wensel, T. G., Baylor, D. A., and Simon, M. I. (2000) Slowed recovery of rod photoresponse in mice lacking the GTPase accelerating protein RGS9-1, *Nature 403*, 557.
34. Chen, C. K., Eversole-Cire, P., Zhang, H., Mancino, V., Chen, Y. J., He, W., Wensel, T. G., and Simon, M. I. (2003) Instability of GGL domain-containing RGS proteins in mice lacking the G protein beta-subunit Gbeta5, *Proc. Natl. Acad. Sci. U.S.A. 100*, 6604.
35. Chase, D. L., Patikoglou, G. A., and Koelle, M. R. (2001) Two RGS proteins that inhibit Galpha(o) and Galpha(q) signaling in

C. elegans neurons require a Gbeta(5)-like subunit for function, *Curr. Biol. 11*, 222.
36. Ponting, C. P., and Bork, P. (1996) Pleckstrin's repeat performance: a novel domain in G-protein signaling?, *Trends Biochem. Sci. 21*, 245.
37. Wong, H. C., Mao, J., Nguyen, J. T., Srinivas, S., Zhang, W., Liu, B., Li, L., Wu, D., and Zheng, J. (2000) Structural basis of the recognition of the dishevelled DEP domain in the Wnt signaling pathway, *Nat. Struct. Biol. 7*, 1178.
38. Civera, C., Simon, B., Stier, G., Sattler, M., and Macias, M. J. (2005) Structure and dynamics of the human pleckstrin DEP domain: distinct molecular features of a novel DEP domain subfamily, *Proteins 58*, 354.
39. Hepler, J. R. (2005) R7BP: a surprising new link between G proteins, RGS proteins, and nuclear signaling in the brain, *Sci. STKE 2005*, pe38.
40. Hu, G., Zhang, Z., and Wensel, T. G. (2003) Activation of RGS9-1 GTPase acceleration by its membrane anchor, R9AP, *J. Biol. Chem. 278*, 14550.
41. Martemyanov, K. A., Lishko, P. V., Calero, N., Keresztes, G., Sokolov, M., Strissel, K. J., Leskov, I. B., Hopp, J. A., Kolesnikov, A. V., Chen, C. K., Lem, J., Heller, S., Burns, M. E., and Arshavsky, V. Y. (2003) The DEP domain determines subcellular targeting of the GTPase activating protein RGS9 in vivo, *J. Neurosci. 23*, 10175.
42. Drenan, R. M., Doupnik, C. A., Boyle, M. P., Muglia, L. J., Huettner, J. E., Linder, M. E., and Blumer, K. J. (2005) Palmitoylation regulates plasma membrane-nuclear shuttling of R7BP, a novel membrane anchor for the RGS7 family, *J. Cell Biol. 169*, 623.
43. Hunt, R. A., Edris, W., Chanda, P. K., Nieuwenhuijsen, B., and Young, K. H. (2003) Snapin interacts with the N-terminus of regulator of G protein signaling 7, *Biochem. Biophys. Res. Commun. 303*, 594.
44. Levay, K., Satpaev, D. K., Pronin, A. N., Benovic, J. L., and Slepak, V. Z. (1998) Localization of the sites for Ca^{2+}-binding proteins on G protein-coupled receptor kinases, *Biochemistry 37*, 13650.
45. Witherow, D. S., and Slepak, V. Z. (2004) Biochemical purification and functional analysis of complexes between the G-protein subunit Gbeta5 and RGS proteins, *Methods Enzymol. 390*, 149.
46. Clapham, D. E., and Neer, E. J. (1997) G protein beta gamma subunits, *Annu. Rev. Pharmacol. Toxicol. 37*, 167.
47. Hamm, H. E. (1998) The many faces of G protein signaling, *J. Biol. Chem. 273*, 669.
48. Schwindinger, W. F., and Robishaw, J. D. (2001) Heterotrimeric G-protein betagamma-dimers in growth and differentiation, *Oncogene 20*, 1653.
49. Dell, E. J., Connor, J., Chen, S., Stebbins, E. G., Skiba, N. P., Mochly-Rosen, D., and Hamm, H. E. (2002) The betagamma subunit of heterotrimeric G proteins interacts with RACK1 and two other WD repeat proteins, *J. Biol. Chem. 277*, 49888.
50. Simonds, W. F., Butrynski, J. E., Gautam, N., Unson, C. G., and Spiegel, A. M. (1991) G-protein, beta gamma dimers. Membrane targeting requires subunit coexpression and intact gamma C-A-A-X domain, *J. Biol. Chem. 266*, 5363.
51. Takida, S., and Wedegaertner, P. B. (2003) Heterotrimer formation, together with isoprenylation, is required for plasma membrane targeting of Gbetagamma, *J. Biol. Chem. 278*, 17284.
52. Yoshikawa, D. M., Hatwar, M., and Smrcka, A. V. (2000) G protein beta 5 subunit interactions with alpha subunits and effectors, *Biochemistry 39*, 11340.
53. Bayewitch, M. L., Avidor-Reiss, T., Levy, R., Pfeuffer, T., Nevo, I., Simonds, W. F., and Vogel, Z. (1998) Inhibition of adenylyl cyclase isoforms V and VI by various Gbetagamma subunits, *FASEB J. 12*, 1019.
54. Lei, Q., Jones, M. B., Talley, E. M., Garrison, J. C., and Bayliss, D. A. (2003) Molecular mechanisms mediating inhibition of G protein-coupled inwardly-rectifying K^+ channels, *Mol. Cells 15*, 1.
55. Rose, J. J., Taylor, J. B., Shi, J., Cockett, M. I., Jones, P. G., and Hepler, J. R. (2000) RGS7 is palmitoylated and exists as biochemically distinct forms, *J. Neurochem. 75*, 2103.
56. Patikoglou, G. A., and Koelle, M. R. (2002) An N-terminal region of *Caenorhabditis elegans* RGS proteins EGL-10 and EAT-16 directs inhibition of G(alpha)o versus G(alpha)q signaling, *J. Biol. Chem. 277*, 47004.
57. Zhang, J. H., Barr, V. A., Mo, Y., Rojkova, A. M., Liu, S., and Simonds, W. F. (2001) Nuclear localization of G protein beta 5 and regulator of G protein signaling 7 in neurons and brain, *J. Biol. Chem. 276*, 10284.
58. Rojkova, A. M., Woodard, G. E., Huang, T. C., Combs, C. A., Zhang, J. H., and Simonds, W. F. (2003) Ggamma subunit-selective G protein beta 5 mutant defines regulators of G protein signaling protein binding requirement for nuclear localization, *J. Biol. Chem. 278*, 12507.
59. Gerachshenko, T., Blackmer, T., Yoon, E. J., Bartleson, C., Hamm, H. E., and Alford, S. (2005) Gbetagamma acts at the C terminus of SNAP-25 to mediate presynaptic inhibition, *Nat. Neurosci. 8*, 597.
60. Blackmer, T., Larsen, E. C., Bartleson, C., Kowalchyk, J. A., Yoon, E. J., Preininger, A. M., Alford, S., Hamm, H. E., and Martin, T. F. (2005) G protein betagamma directly regulates SNARE protein fusion machinery for secretory granule exocytosis, *Nat. Neurosci. 8*, 421.
61. Katoh, K., Kuma, K., Toh, H., and Miyata, T. (2005) MAFFT version 5: improvement in accuracy of multiple sequence alignment, *Nucleic Acids Res. 33*, 511.
62. Katoh, K., Misawa, K., Kuma, K., and Miyata, T. (2002) MAFFT: a novel method for rapid multiple sequence alignment based on fast Fourier transform, *Nucleic Acids Res. 30*, 3059.
63. Gouet, P., Courcelle, E., Stuart, D. I., and Metoz, F. (1999) ESPript: analysis of multiple sequence alignments in PostScript, *Bioinformatics 15*, 305.

BI700524W